Enhanced Energy Detection for Multi-band Spectrum Sensing under RF Imperfections

Ahmet Gokceoglu, Sener Dikmese, Mikko Valkama, and Markku Renfors

Department of Electronics and Communications Engineering
Tampere University of Technology
Korkeakoulunkatu 1, FI-33720, Tampere, FINLAND
{ahmet.gokceoglu, sener.dikmese, mikko.e.valkama, markku.renfors}@tut.fi

Abstract— **In this paper, we study simultaneous multi-channel spectrum sensing in cognitive radio context. The sensing receiver RF front-end is assumed to deploy wideband multi-channel IQ down-conversion which is well-suited for highly-integrated circuit implementations. Such RF front-end is, however, also prone to several RF impairments, such as IQ imbalance, which leads to mirror-frequency cross-talk and can thus considerably degrade the sensing performance. Assuming that the individual channel sensing is building on energy detection, we first analyze the spectrum sensing performance of the multichannel sensing receiver in terms of false alarm and detection probabilities. The analysis shows that IQ imbalance is especially harmful in terms of false alarms stemming from the mirror-channel crosstalk, and is greatly emphasized when the overall down-converted signal has high dynamic range. Motivated by this, we present an efficient digital compensation scheme, called *energy correction* method, where the sensing statistics of any particular channel are properly adjusted based on the corresponding mirror-channel statistics such that the effect of the crosstalk is minimized. Optimum minimum mean-squared error (MMSE) solution for the energy correction processing is first derived, complemented then with a practical low-complexity sample estimator. Extensive computer simulations demonstrate that under various parameter settings for IQ imbalance and receiver dynamic range, the proposed scheme yields sensing performance practically identical to the IQ imbalance free reference performance. Thus the proposed method offers feasible RF impairment -aware energy detection solution for practical multichannel sensing receivers.**

Keywords— Energy detection, IQ imbalance, multi-band direct conversion receiver, multi-band spectrum sensing, RF impairments.

I. INTRODUCTION

The available spectrum for wireless communication is a scarce and limited source and hence more efficient utilization of the temporally and/or spatially available spectrum chunks is one of the most important challenges in the evolution of wireless systems and radio devices [1]. In order to improve the utilization of the available spectrum, the concept of cognitive radio (CR) has been introduced [2] and is under active research. One of the most important tasks of CR devices is to identify the spatially and/or temporally available spectral chunks which is generally referred to as spectrum sensing. Over the recent past, a great deal of efforts has been put to derive optimal, suboptimal and ad-hoc solutions to the spectrum sensing problem, see, e.g., [3] and [4] and the references therein. Among the various methods, one of the most well-known approach is the classical energy detection (ED).

While majority of the work in spectrum sensing field has focused on deploying detection theoretic tools to the sensing task, CR devices as a whole are *fundamentally RF devices* and thus as any receiver, contain the *RF front-end* and analog-digital (A/D) interface prior to digital signal processing. So far, most of the algorithmic spectrum sensing studies have neglected the implementation challenges and RF imperfections associated to the RF front-end, even though the large dynamic range a CR device has to cope with calls for high linearity and spurious free dynamic range in the RF parts. Among the very few previous works, [5] and [6] point out these RF challenges in broadband sensing and discusses the importance of improved front-end linearity and sensitivity at general level. Another work that studies the RF front-end imperfections in context of wideband CR applications is [7] where the impacts of non-linearities due to low noise amplifiers (LNA), mixers or IF-amplifiers (IF-A) are demonstrated and a feedforward linearization technique is proposed. In [8], impacts of IQ imbalance and sampling frequency offset on several sensing algorithms are discussed, however, the considered model and analysis is limited to narrowband single-channel sensing receiver only and hence does not address the associated problems in broadband multi-channel sensing which is the theme of this article. In [9], in basic single-channel OFDM scenario, the impacts of phase noise, carrier frequency offset and IQ imbalance on cyclostationary based detection are studied.

In this article, we consider simultaneous multichannel energy detection task in a CR receiver deploying wideband I/Q down-conversion based RF front-end that in practice is known to suffer from IQ imbalance and the associated mirror-frequency interference [11]-[13]. Under this receiver setting, Section II presents the essential signal models and analyses the impact of IQ imbalance and associated mirror-frequency cross-talk on the false alarm and detection probabilities in the wideband sensing receiver. In Section III, an efficient mitigation technique, called *statistics level energy correction*, is then proposed to effectively suppress the false alarms stemming from mirror-frequency cross-talk. Optimum correction coefficient together with a practical sample estimator are developed and formulated. Simulation results and discussion are provided in

Section IV illustrating and verifying the excellent processing gain of the proposed mitigation technique in terms of the sensing performance. Finally conclusions are drawn in Section IV.

In order to clarify the used notation throughout the paper, the superscripts *, T and † denote conjugation, transposition and conjugate-transposition operations, respectively. The vector variables are distinguished from scalar ones using bold letters. The operator $\mathrm{Re}\{.\}$ returns the real part of a complex variable whereas $E[.]$ stands for expectation operator. The subscripts indicate the conditioning random variables, e.g. $\mu_\theta(k)$ denotes $\mu(k)$ being conditioned on θ. The only exception to this rule is for the variable k which is reserved for channel index. In that case, the conditioning random variables are distinguished with the use of bar symbol $|$, e.g. $y_{k|\theta}(n)$.

II. Fundemental Signal and System Models

As already mentioned, we assume that a collection of RF channels to be sensed is IQ down-converted simultaneously to lower frequencies. This is illustrated in Figure 1. The CR device then does separate energy detection in parallel for each channel and decides whether the channels are occupied by a primary user (PU) or not. The overall multichannel down-conversion principle, together with mirror-channel crosstalk due to IQ imbalance, are illustrated in Figure 1 where each channel has interference from its mirror or image channel.

For notational convenience, we now enumerate the channels as $S_K = \{-K,\cdots,-1,1,\cdots,K\}$ where $K = 3$ in the example scenario illustrated in Figure 1. In this particular scenario, PU1 at channel -1 is interfered with the image of PU2, and vice versa. In addition, the spectral hole at channel $k = -3$ is interfered with the mirror image of PU3. Obviously, if there is a strong signal at the image channel, then there is considerable interference to the primary channel which is being sensed. In the next subsection, starting from the ideal RF scenario, we will present the fundamental received signal models as well as derive the false alarm and detection probabilities under IQ imbalance. These are then used as a basis in Section III to develop the actual enhanced energy detection scheme suppressing the effects of the mirror-channel cross-talk efficiently in the sensing statistics.

A. Signal Models

The ideal (zero IQ imbalance) baseband equivalent received signal model for an arbitrary channel k is given by

$$y^{\text{ideal}}_{k|\theta}(n) = \theta x_k(n) + w_k(n) \tag{1}$$

where $x_k(n)$ and $w_k(n)$ denote PU signal and receiver noise processes, sampled at time time instant n, and the parameter $\theta \in \{0,1\}$ indicates the detection hypothesis 0 or 1. Thus when $\theta = 0$, the first term on right hand side disappears leaving only the receiver noise whereas for $\theta = 1$ both the PU signal and the receiver noise are present. On the other hand, the IQ imbalanced signal model with interference from the image channel $-k$, as illustrated in Figure 1, can be formulated as

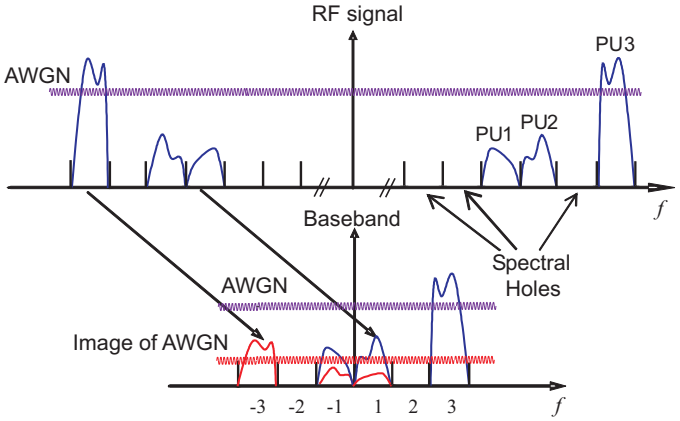

Figure 1: Illustration of multichannel IQ down-conversion principle and the associated mirror-frequency cross-talk due to IQ imbalance.

$$y^{\text{IQ}}_{k|\theta,\xi}(n) = g_1(\theta x_k(n) + w_k(n)) + g_2(\xi x_{-k}(n) + w_{-k}(n))^* \tag{2}$$

where $x_{-k}(n)$ and $w_{-k}(n)$ are the image channel PU and receiver noise processes, sampled at time time instant n, $g_1 = (1+\rho e^{-j\phi})/2$, $g_2 = (1-\rho e^{j\phi})/2$ with ρ and ϕ denoting the actual amplitude and phase imbalances and the parameter $\xi \in \{0,1\}$ indicates the existence of a PU signal at the image channel. Notice also that setting $g_1 = 1$ and $g_2 = 0$ (or $\rho = 1$ and $\phi = 0$) in (2) gives the ideal signal model. Intuitively, the sensing performance of the primary channel is essentially affected only if there is considerable mirror-channel interference, thus in the following we will mostly focus on the case $\xi = 1$. Hence, the general signal model in (2) and the associated sensing statistics and performance will be studied further in the presence of the image channel PU signal and thus ξ is omitted in the upcoming notations. The signal model can then be written as

$$y^{\text{IQ}}_{k|\theta}(n) = g_1(\theta x_k(n) + w_k(n)) + g_2(x_{-k}(n) + w_{-k}(n))^* \tag{3}$$

As an example, the scenario illustrated for the channel $k = -3$ in Figure 1 corresponds to the model (3) with $\theta = 0$ but with interference coming from the image channel $k = 3$.

In the following, we will further assume that $w_k(n)$, $x_k(n)$, $w_{-k}(n)$, and $x_{-k}(n)$ are all mutually independent zero-mean circularly symmetric complex Gaussian variables with variances $\sigma^2_w(k) = E[|w_k(n)|^2]$, $\sigma^2_x(k) = E[|x_k(n)|^2]$, $\sigma^2_w(-k) = E[|w_{-k}(n)|^2]$ and $\sigma^2_x(-k) = E[|x_{-k}(n)|^2]$, respectively. Without loss of generality, we will assume that the receiver noise variances are identical for all channels, i.e., $\sigma^2_w(k) = \sigma^2_w(-k) = \sigma^2_w$. For further use, we define the following $N \times 1$ vectors

$$\begin{aligned} \mathbf{w}_k &= [w_k(n), w_k(n-1), \cdots, w_k(n-N+1)]^T \\ \mathbf{x}_k &= [x_k(n), x_k(n-1), \cdots, x_k(n-N+1)]^T \end{aligned} \tag{4}$$

Then, the received observation vectors for channel k and $-k$ under ideal RF read

$$\mathbf{y}^{\text{ideal}}_{k|\theta} = \theta \mathbf{x}_k + \mathbf{w}_k, \quad \mathbf{y}^{\text{ideal}}_{-k} = \mathbf{x}_{-k} + \mathbf{w}_{-k} \tag{5}$$

Correspondingly, the IQ imbalanced received signal vectors conditioned on hypothesis $\theta \in \{0,1\}$ read

$$\begin{aligned}\mathbf{y}_{k|\theta}^{\mathrm{IQ}} &= g_1\mathbf{y}_{k|\theta}^{\mathrm{ideal}} + g_2\left(\mathbf{y}_{-k}^{\mathrm{ideal}}\right)^* \\ \mathbf{y}_{-k|\theta}^{\mathrm{IQ}} &= g_1\mathbf{y}_{-k}^{\mathrm{ideal}} + g_2\left(\mathbf{y}_{k|\theta}^{\mathrm{ideal}}\right)^*\end{aligned} \tag{6}$$

Next, in the following subsection, we use these signal models to analytically analyze the false alarm and detection probabilities of an arbitrary primary channel suffering from the image channel interference.

B. False Alarm and Detection Probabilities

The energy detector with ideal RF calculates the sample energy for channel k as

$$T^{\mathrm{ideal}}(k) = \left(\mathbf{y}_k^{\mathrm{ideal}}\right)^{\dagger}\mathbf{y}_k^{\mathrm{ideal}} \tag{7}$$

and compares it to a threshold for making a decision i.e., channel k is available if $T^{\mathrm{ideal}}(k) < \gamma^{\mathrm{ideal}}$ and not available otherwise. For large N, the distribution of (7) is often approximated [3] as Gaussian distribution with mean $\mu_\theta^{\mathrm{ideal}}(k)$ and variance $v_\theta^{\mathrm{ideal}}(k)$ which are given as

$$\mu_\theta^{\mathrm{ideal}}(k) = \theta\sigma_x^2(k) + \sigma_w^2,\ v_\theta^{\mathrm{ideal}}(k) = \frac{(\mu_\theta^{\mathrm{ideal}}(k))^2}{N} \tag{8}$$

The corresponding false alarm and detection probabilities are then obtained by using the standard Q-function as

$$P_{fa}^{\mathrm{ideal}}(k) \simeq Q\left(\frac{\gamma^{\mathrm{ideal}} - \mu_0^{\mathrm{ideal}}(k)}{\sqrt{v_0^{\mathrm{ideal}}(k)}}\right) = Q\left(\frac{\gamma^{\mathrm{ideal}} - \mu_0^{\mathrm{ideal}}(k)}{\mu_0^{\mathrm{ideal}}(k)\,/\,\sqrt{N}}\right) \tag{9}$$

$$P_{d}^{\mathrm{ideal}}(k) \simeq Q\left(\frac{\gamma^{\mathrm{ideal}} - \mu_1^{\mathrm{ideal}}(k)}{\sqrt{v_1^{\mathrm{ideal}}(k)}}\right) = Q\left(\frac{\gamma^{\mathrm{ideal}} - \mu_1^{\mathrm{ideal}}(k)}{\mu_1^{\mathrm{ideal}}(k)\,/\,\sqrt{N}}\right) \tag{10}$$

For a target false alarm probability, P_{fa}^{trgt}, the threshold can be solved from (9) as

$$\gamma^{\mathrm{ideal}} = \sigma_w^2 + \frac{Q^{-1}(P_{fa}^{\mathrm{trgt}})\sigma_w^2}{\sqrt{N}} \tag{11}$$

Note that in practice the CR device has certain noise measurements and has only an estimate for the receiver noise variance $\mu_0^{\mathrm{ideal}}(k) = \sigma_w^2$. In all the following analysis, however, we will assume that the receiver has perfect knowledge on the receiver noise variance which is obtained from calibration measurements. This assumption is done in order to be able to quantify the performance degradation due to considered RF IQ imbalance, independently of the classical noise uncertainty problem.

Under IQ imbalanced model, the energy detector with ideal RF calculates the sample energy for channel k as

$$\begin{aligned}T^{\mathrm{IQ}}(k) &= \left(\mathbf{y}_k^{\mathrm{IQ}}\right)^{\dagger}\mathbf{y}_k^{\mathrm{IQ}} \\ &= \left|g_1\right|^2 T^{\mathrm{ideal}}(k) + \left|g_2\right|^2 T^{\mathrm{ideal}}(-k) \\ &\quad + 2\,\mathrm{Re}\left\{g_1 g_2^* R(k)\right\}\end{aligned} \tag{12}$$

where $R(k) = \left(\mathbf{y}_k^{\mathrm{ideal}}\right)^T \mathbf{y}_{-k}^{\mathrm{ideal}}$. Again for large N, the distribution of (12) can be approximated with Gaussian distribution with mean $\mu_\theta^{\mathrm{IQ}}(k)$ and variance $v_\theta^{\mathrm{IQ}}(k)$ which are given as

$$\begin{aligned}\mu_\theta^{\mathrm{IQ}}(k) &= \left|g_1\right|^2 \mu_\theta^{\mathrm{ideal}}(k) + \left|g_2\right|^2 \mu_1^{\mathrm{ideal}}(-k) \\ v_\theta^{\mathrm{IQ}}(k) &= \frac{(\mu_\theta^{\mathrm{IQ}}(k))^2}{N}\end{aligned} \tag{13}$$

Correspondingly, the detection and false alarm probabilities of the imbalanced model are given by

$$P_{fa}^{\mathrm{IQ}}(k) \simeq Q\left(\frac{\gamma^{\mathrm{IQ}} - \mu_0^{\mathrm{IQ}}(k)}{\sqrt{v_0^{\mathrm{IQ}}(k)}}\right) = Q\left(\frac{\gamma^{\mathrm{IQ}} - \mu_0^{\mathrm{IQ}}(k)}{\mu_0^{\mathrm{IQ}}(k)\,/\,\sqrt{N}}\right) \tag{14}$$

$$P_{d}^{\mathrm{IQ}}(k) \simeq Q\left(\frac{\gamma^{\mathrm{IQ}} - \mu_1^{\mathrm{IQ}}(k)}{\sqrt{v_1^{\mathrm{IQ}}(k)}}\right) = Q\left(\frac{\gamma^{\mathrm{IQ}} - \mu_1^{\mathrm{IQ}}(k)}{\mu_1^{\mathrm{IQ}}(k)\,/\,\sqrt{N}}\right) \tag{15}$$

where γ^{IQ} denotes the deployed threshold. Again, we consider that the CR device has perfect knowledge on the variance of receiver noise process $g_1 w_k(n) + g_2(w_{-k}(n))^*$. This is physically plausible implying simply that the same receiver hardware is used in the noise calibration measurements, as in the actual sensing period. Then the deployed threshold read

$$\gamma^{\mathrm{IQ}} = (\left|g_1\right|^2 + \left|g_2\right|^2)\sigma_w^2 + \frac{Q^{-1}(P_{fa}^{\mathrm{trgt}})(\left|g_1\right|^2 + \left|g_2\right|^2)\sigma_w^2}{\sqrt{N}} \tag{16}$$

Since the receiver knowledge is limited to noise variance only, i.e., to $(\left|g_1\right|^2 + \left|g_2\right|^2)\sigma_w^2$, and is assumed to have no further knowledge of IQ imbalance parameters or image channel signal, the receiver is uncertain about the exact value of the prevailing total noise floor $\mu_0^{\mathrm{IQ}}(k)$. This leads to the well-known SNR-wall problem discussed e.g. in [10], and is one interpretation of the IQ imbalance problem in multichannel receivers.

Note that, comparing (14) and (9), for any positive image channel PU signal power $\sigma_x^2(-k) > 0$, we have $P_{fa}^{\mathrm{IQ}}(k) > P_{fa}^{\mathrm{ideal}}(k)$. For fixed IQ imbalance, $\mu_0^{\mathrm{IQ}}(k)$ monotonically increases with increasing $\sigma_x^2(-k)$, and so does the $P_{fa}^{\mathrm{IQ}}(k)$. Now defining the signal-to-interference ratio $SIR := \sigma_x^2(-k)\,/\,\sigma_x^2(k)$ and by comparing (15) and (10), it can be shown that $P_d^{\mathrm{IQ}}(k) > P_d^{\mathrm{ideal}}(k)$ if $SIR < 1$. Conversely, $P_d^{\mathrm{IQ}}(k) < P_d^{\mathrm{ideal}}(k)$ for $SIR > 1$ which is the case where both false alarm and detection probabilities are worse for the IQ imbalanced model compared to ideal RF. Yet, considering practical IQ imbalance value with typical image rejection ratios in the order of 30-40 dB, the concerned cases are $SIR \ll 1$ such that $P_d^{\mathrm{IQ}}(k) > P_d^{\mathrm{ideal}}(k)$. This increase in detection probability, however, comes with a price of increased false alarm probability, i.e., $P_{fa}^{\mathrm{IQ}}(k) > P_{fa}^{\mathrm{ideal}}(k)$. This decrease in the ability to identify available channels is the main motivation of the compensation method which will be proposed next.

III. Enhanced Energy Detection with RF IQ Imbalance Suppression

As presented in the previous section, IQ imbalance leads to an increase in the false alarm probability thus decreasing the op-

portunities for SU to access vacant channels. In this section, we formulate a compensation scheme for enhanced spectrum sensing that aims to achieve false alarm probabilities close to those of the ideal signal model. Furthermore, since the detection probability is the highest priority performance metric, the proposed compensation schemes are developed such that the detection probabilities are essentially identical to the ideal signal model case. In general, the CR device can decide whether or not to apply the suppression methods at a particular sensing channel based on prevailing image band statistics. Thus we assume that classical sample energy statistics are first accumulated for each channel, as would be done anyway if simultaneous sensing of multiple channels is deployed. Then, if the image band statistics of any particular channel is clearly above the receiver noise variance of that channel, i.e., $T^{\mathrm{IQ}}(-k) \gg (\left|g_1\right|^2 + \left|g_2\right|^2)\sigma_w^2$, then the following enhancement scheme can and should be applied to prevent degradation in false alarm probability and the resulting loss in spectrum utilization.

A. Proposed Energy Correction Principle

In the literature, extensive work has been carried out for IQ imbalance compensation in classical receiver context for enhancing the demodulation performance under IQ imbalance. Good example is the waveform or sample level interference cancellation scheme, proposed originally in [13], that subtracts a scaled image channel signal from primary channel signal to suppress interference. Also various alternative methods have been proposed suppressing the image interference at sample level. On the other hand, the spectrum sensing task is only dependent on the *quality of the associated test statistics*. Thus as long as the key features of the statistics remain unaffected, everything else is secondary. This motivates for a correction method that works directly on the primary and image channel statistics, instead of trying to clean the signals or waveforms explicitly. In this respect, the *corrected statistics* is obtained as

$$\begin{aligned} T^{\mathrm{EC}}(k) &= T^{\mathrm{IQ}}(k) - \alpha T^{\mathrm{IQ}}(-k) \\ &= \left|g_1^{\mathrm{EC}}\right|^2 T^{\mathrm{ideal}}(k) + \left|g_2^{\mathrm{EC}}\right|^2 T^{\mathrm{ideal}}(-k) \\ &\quad +2(1-\alpha)\,\mathrm{Re}\{g_1 g_2^* R(k)\} \end{aligned} \tag{17}$$

In above, $\alpha \in \mathbb{R}$ is the correction coefficient, $\left|g_1^{\mathrm{EC}}\right|^2 = |g_1|^2 - \alpha|g_2|^2$ and $\left|g_2^{\mathrm{EC}}\right|^2 = |g_2|^2 - \alpha|g_1|^2$. The distribution of *corrected statistics* in (17) can be accurately approximated with Gaussian distribution having mean $\mu_\theta^{\mathrm{EC}}(k)$ and variance $v_\theta^{\mathrm{EC}}(k)$ written explicitly as

$$\begin{aligned} \mu_\theta^{\mathrm{EC}}(k) &= \left|g_1^{\mathrm{EC}}\right|^2 \mu_\theta^{\mathrm{ideal}}(k) + \left|g_2^{\mathrm{EC}}\right|^2 \mu_1^{\mathrm{ideal}}(-k) \\ v_\theta^{\mathrm{EC}}(k) &= \frac{1}{N}\Big(\left|g_1^{\mathrm{EC}}\right|^2 (\mu_\theta^{\mathrm{ideal}}(k))^2 + \left|g_2^{\mathrm{EC}}\right|^2 (\mu_1^{\mathrm{ideal}}(-k))^2 \\ &\quad +2(1-\alpha)^2 \left|g_1\right|^2 \left|g_2\right|^2 \mu_\theta^{\mathrm{ideal}}(k)\mu_1^{\mathrm{ideal}}(-k)\Big) \end{aligned} \tag{18}$$

Corresponding detection and false alarm probabilities are then

$$P_{fa}^{\mathrm{EC}}(k) \simeq Q\left(\frac{\gamma - \mu_0^{\mathrm{EC}}(k)}{\sqrt{v_0^{\mathrm{EC}}(k)}}\right), \quad P_d^{\mathrm{EC}}(k) \simeq Q\left(\frac{\gamma - \mu_1^{\mathrm{EC}}(k)}{\sqrt{v_1^{\mathrm{EC}}(k)}}\right) \tag{19}$$

B. Optimum MMSE Correction Coefficient and Practical Sample Estimator

To find an appropriate correction coefficient α, the widely-used minimum mean squared error (MMSE) criterion is deployed. The cost function to be minimized is thus

$$J_\theta(\alpha) = E\left[\left|T_\theta^{\mathrm{ideal}}(k) - T_\theta^{\mathrm{EC}}(k)\right|^2\right] = a_\theta \alpha^2 + b_\theta \alpha + c_\theta \tag{20}$$

In above, the coefficients of the quadratic form are given by

$$\begin{aligned} a_\theta &= M_1(\left|g_2\right|^4 (\mu_\theta^{\mathrm{ideal}}(k))^2 + \left|g_1\right|^4 (\mu_1^{\mathrm{ideal}}(-k))^2 \\ &\quad +2\left|g_1\right|^2 \left|g_2\right|^2 \mu_\theta^{\mathrm{ideal}}(k)\mu_1^{\mathrm{ideal}}(-k)) \\ b_\theta &= 2M_1(\left|g_2\right|^2 (1-\left|g_1\right|^2)(\mu_\theta^{\mathrm{ideal}}(k))^2 - \left|g_1 g_2\right|^2 (\mu_1^{\mathrm{ideal}}(-k))^2) \\ &\quad +2\mu_\theta^{\mathrm{ideal}}(k)\mu_1^{\mathrm{ideal}}(-k)(\left|g_1\right|^2 (1-2M_2\left|g_2\right|^2 - \left|g_1\right|^2) - \left|g_2\right|^4) \\ c_\theta &= M_1((1-\left|g_1\right|^2)^2 (\mu_\theta^{\mathrm{ideal}}(k))^2 + \left|g_2\right|^4 (\mu_1^{\mathrm{ideal}}(-k))^2) \\ &\quad +2\mu_\theta^{\mathrm{ideal}}(k)\mu_1^{\mathrm{ideal}}(-k)\left|g_2\right|^2 (\left|g_1\right|^2 (1-M_2) - 1) \end{aligned} \tag{21}$$

with $M_1 = (N+1)/N$ and $M_2 = 1/N$. Hence, strictly speaking, the optimum scaling coefficient(s) obtained from the roots of the quadratic form $r_\theta = (-b_\theta \pm \sqrt{b_\theta^2 - 4a_\theta c_\theta})/(2a_\theta)$ depend on hypothesis θ. However, approximating $M_1 \simeq 1$ and $M_2 \simeq 0$, considering that for practical IQ imbalance values $|g_1|^2 \gg |g_2|^2$, and assuming that the image band is occupied by a strong PU signal such that for both $\theta = 0$ and 1 $\left|g_2\right|^2 \mu_1^{\mathrm{ideal}}(-k) \gg (1-\left|g_1\right|^2)\mu_\theta^{\mathrm{ideal}}(k)$ is satisfied, then the coefficients in (21) simplify to $a \simeq \left|g_1\right|^4 (\mu_1^{\mathrm{ideal}}(-k))^2$, $b \simeq -2\left|g_1\right|^2 \left|g_2\right|^2 (\mu_1^{\mathrm{ideal}}(-k))^2$ and $c \simeq \left|g_2\right|^4 (\mu_1^{\mathrm{ideal}}(-k))^2$. Therefore, there is only a single root independent of θ, yielding

$$\alpha_{\mathrm{opt}} \simeq \left|g_2\right|^2 / \left|g_1\right|^2 \tag{22}$$

For practical IQ imbalance values and strong image channel signal, a good estimate for the above optimum MMSE coefficient in (22) can be obtained as

$$\alpha_{\mathrm{est}} = |\beta|^2 \tag{23}$$

where β denotes the following sample estimator of the form

$$\beta = \frac{(\mathbf{y}_k^{\mathrm{IQ}})^T \mathbf{y}_{-k}^{\mathrm{IQ}}}{T^{\mathrm{IQ}}(-k)} \simeq \frac{g_2}{g_1^*} \tag{24}$$

While the denominator $T^{\mathrm{IQ}}(-k)$ is directly the image channel sample energy, and thus already available, the numerator needs only N multiplications and $N-1$ additions. Considering the correction operation in (17) requires only one more multiplication and addition, the computational complexity of the above sample estimator is overall more than feasible.

When optimum correction coefficient in (22) is used, then the mean and variance expressions in (18) simplify to

$$\mu_\theta^{\mathrm{EC}}(k) \simeq \left|g_1\right|^2 \mu_\theta^{\mathrm{ideal}}(k)$$
$$v_\theta^{\mathrm{EC}}(k) \simeq \frac{\left|g_1\right|^4 (\mu_\theta^{\mathrm{ideal}}(k))^2 + 2\left|g_1\right|^2 \left|g_2\right|^2 \mu_\theta^{\mathrm{ideal}}(k)\mu_1^{\mathrm{ideal}}(-k)}{N} \quad (25)$$
$$\simeq \frac{\left|g_1\right|^4 (\mu_\theta^{\mathrm{ideal}}(k))^2}{N} = \left|g_1\right|^4 v_\theta^{\mathrm{ideal}}(k)$$

The very last approximation is valid only when $\left|g_2\right|^2 \mu_1^{\mathrm{ideal}}(-k) \ll \mu_\theta^{\mathrm{ideal}}(k)$ which roughly states that the leaked energy from the image channel is considerably below the energy of that particular channel. Although we have been concerned with the scenarios where image channel is occupied with a strong PU signal, the leaked power can be, say 10 dB below the receiver noise variance and yet still causing considerable degradation in false alarm performance. Considering typical IQ imbalance with image rejection ratios in the order of 30-40 dB, the above approximation is accurate for image channel PU signal powers up to 20-30 dB which is still in-line with the assumed scenario. Consequently, under optimum coefficient setting, the mean and variance of the *corrected statistics* can be well approximated with mean and variance of ideal RF up to a scaling constant. If the deployed threshold is also the ideal threshold in (11) scaled by $\left|g_1\right|^2$, then the false alarm and detection probabilities in (19) match with (9) and (10). In order to have such scaling for the threshold, the noise measurements for channel k and $-k$ can be used to obtain

$$\mu_0^{\mathrm{EC}}(k) = \mu_0^{\mathrm{IQ}}(k) - \alpha_{\mathrm{opt}}\mu_0^{\mathrm{IQ}}(k) \simeq \left|g_1\right|^2 \mu_0^{\mathrm{ideal}}(k) = \left|g_1\right|^2 \sigma_w^2 \quad (26)$$

which in turn can be used to get the desired threshold as

$$\gamma^{\mathrm{EC}} = \mu_0^{\mathrm{EC}}(k) + \frac{Q^{-1}(P_{fa}^{\mathrm{trgt}})\mu_0^{\mathrm{EC}}(k)}{N} \simeq \left|g_1\right|^2 \gamma^{\mathrm{ideal}} \quad (27)$$

Yet more practically, the estimated coefficient in (23) is to be used instead of the optimum coefficient given by (22). It is more challenging to argue, though, that the mean and variance of the *corrected statistics* are related to mean and variance of ideal RF through simple scaling when the practical sample estimator in (24) is used for the correction coefficient. However, when the image band is occupied by strong PU signal such that the estimation is good, it is found that such relation exist with a scaling coefficient being approximately $\left|g_1\right|^2 - 2\left|g_2\right|^2$. Then, for the proper scaling of threshold, the noise measurements for channel k and $-k$ can be used to obtain first

$$\mu_0^{\mathrm{EC}}(k) = \mu_0^{\mathrm{IQ}}(k) - 3\alpha_{\mathrm{est}}\mu_0^{\mathrm{IQ}}(k) \simeq (\left|g_1\right|^2 - 2\left|g_2\right|^2)\sigma_w^2 \quad (28)$$

Then (28) should be used in (27) to get the desired threshold.

IV. Simulation Results and Discussions

In all simulations, number of samples and target false alarm probability are set to $N = 10^4$ and $P_{fa}^{\mathrm{trgt}} = 0.1$, respectively whereas the results are averaged over 10^4 independent Monte-Carlo simulations. The thresholds are set by plugging (26) and (28) into (27) for operation under $\alpha = \alpha_{\mathrm{opt}}$ and $\alpha = \alpha_{\mathrm{est}}$, respectively. The signal and interference to noise ratios are defined as $SNR := \sigma_x^2(k) \,/\, \sigma_w^2$ and $INR := \sigma_x^2(-k) \,/\, \sigma_w^2$, respectively. The simulated values for ideal RF and *energy correction* with optimum coefficient setting were observed to be practically identical for all INR and IQ imbalance settings. Therefore, same marker is used for these two for better readability.

In Figure 2, the detection probabilities are plotted against SNR for INR of 10, 13 and 16 dB with fixed IQ imbalance of $\rho = 0.99$ and $\phi = 3°$. The detection probabilities corresponding to uncompensated detection are higher compared to those of ideal RF. However, as expected such increase in detection probability comes with a price of increased false alarm probability. The corresponding false alarm probabilities are 0.28, 0.55 and 0.93, respectively which is significantly above the false alarm probability of ideal RF. When the *energy correction* method is applied with optimum coefficient and then with practical sample estimator, the corresponding detection and false alarm probabilities are matching very well with ideal RF. Similar behavior is observed in Figure 3 where detection probabilities are plotted against SNR for $\phi = 3°$, $5°$ and $7°$ with fixed $\rho = 0.99$ and $INR = 10$ dB. This time the *energy correction* method yields slightly higher false alarm probability of 0.11 and 0.14 when the phase imbalances are $5°$ and $7°$, respectively. This is due to above discussion that the estimation in (24) gets better for smaller IQ imbalance values.

In order to further elaborate this behavior, false alarm probabilities are plotted against INR for various amplitude and phase mismatches. The SNR is set to -14 dB such that the corresponding detection probabilities are practically 1 for all curves. It is observed that for INR values lower than 10 dB, the deviation of obtained false alarm probabilities from the target false alarm probability increase with increasing amplitude and phase mismatches. Yet, even for INR as low as 5 dB and IQ imbalance values as high as $\rho = 0.95$ and $\phi = 7°$, the *energy correction* method still achieves lower false alarm probability compared to uncompensated case.

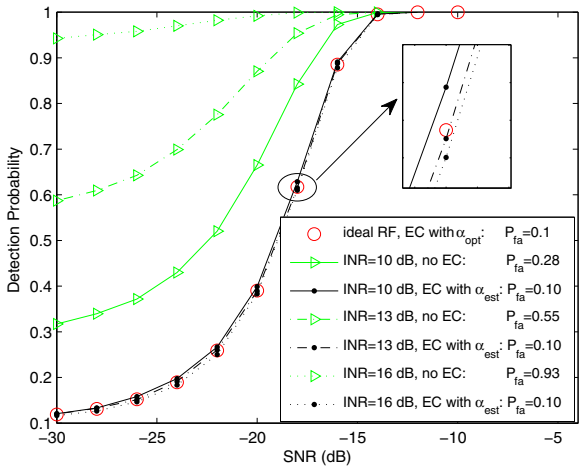

Figure 2: Detection probability vs. SNR. Corresponding false alarm probabilities are reported in the legend. Amplitude and phase imbalances are $\rho = 0.99$ and $\phi = 3°$. Number of samples and target false alarm probability are $N = 10^4$ and $P_{fa}^{\mathrm{trgt}} = 0.1$, respectively.

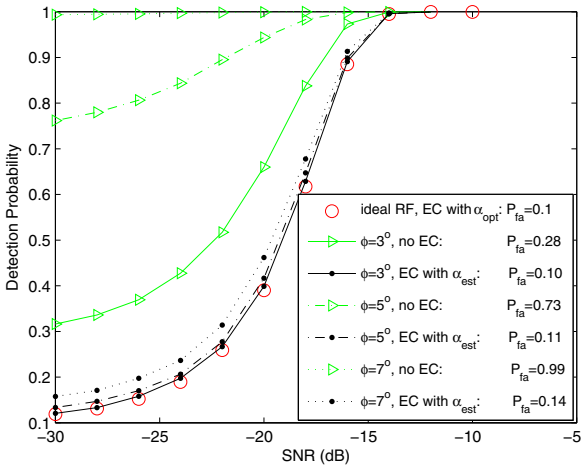

Figure 3: Detection probability vs. SNR . Corresponding false alarm probabilities are reported in the legend. Amplitude imbalance is $\rho = 0.99$ and $INR = 10$ dB. Number of samples and target false alarm probability are $N = 10^4$ and $P_{fa}^{\text{trgt}} = 0.1$, respectively.

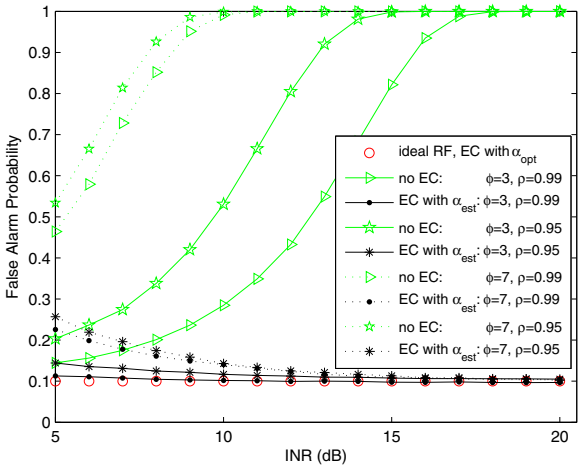

Figure 4: False alarm probability vs. INR when $SNR = -14$ dB such that the corresponding detection probabilities are in the range of $0.995 - 1$ for all curves. Number of samples and target false alarm probability are $N = 10^4$ and $P_{fa}^{\text{trgt}} = 0.1$, respectively.

Overall, the results clearly demonstrate that the proposed enhanced *energy correction* method provides excellent processing gain against mirror-frequency cross-talk in multichannel sensing with very low computational complexity.

V. Conclusions

This article focused on the RF imperfection problematics in wideband CR sensing receivers deploying wideband IQ down-conversion and multichannel energy detection. As shown through detailed analysis and simulations, RF IQ imbalance of the wideband RF front-end degrades the false alarm probability of sensing an arbitrary RF channel significantly when the corresponding image channel has a strong PU signal. To enhance the energy detection in such scenarios, we proposed an *energy correction* method working directly on the sample energy statistics level. The optimum correction coefficient together with practical coefficient estimator using the samples of any particular channel and its image channel were derived. The simulation results demonstrated the good performance of the method, achieving detection and false alarm probabilities practically identical to the ideal RF front-end model under both optimum as well as estimated coefficient settings. Also the computational complexity of the proposed solution is very low, making it feasible for practical devices sensing the RF spectrum with imperfect RF modules.

Acknowledgment

The research leading to these results has been financially supported by the Doctoral Programme of the President of Tampere University of Technology, the Graduate School GETA, the Finnish Funding Agency for Technology and Innovation (Tekes, under the project "Enabling Methods for Dynamic Spectrum Access and Cognitive Radio), the Academy of Finland (under the project 251138 "Digitally-Enhanced RF for Cognitive Radio Devices"), Finnish Foundation for Technology Promotion (TES) and the Austrian Competence Center in Mechatronics (ACCM), all of which are gratefully acknowledged.

References

[1] FCC, Spectrum Policy Task Force Report, ET Docket No. 02-135, November 2002.

[2] I. Mitola, J. and J. Maguire, G. Q., "Cognitive radio: making software radios more personal," *IEEE Personal Commun. Mag.*, vol. 6, no. 4, pp. 13–18, Aug. 1999.

[3] Y. Zeng, Y.C. Liang, A. T. Hoang, and R. Zhang, "A Review on Spectrum Sensing for Cognitive Radio: Challenges and Solutions," *EURASIP Journal Adv. Signal Processing*, vol. 2010, pp. 1-15, Jan. 2010.

[4] T. Yucek and H. Arslan, "A survey of spectrum sensing algorithms for cognitive radio applications," *IEEE Communications Surveys & Tutorials*, vol. 11, no. 1, pp. 116–130, March 2009.

[5] D. Cabric, S. M. Mishra, R. W. Brodersen, "Implementation issues in spectrum sensing for cognitive radios," *Signals, Systems and Computers 2004. Conference Record of the Thirty Eighth Asilomar*, vol.1, pp. 772-776, Nov. 2004

[6] H. Zamat, B. Natarajan, "Use of dedicated broadband sensing receiver in cognitive radio," *IEEE Communications Workshop*, pp. 508-512, May 2008.

[7] M. Grimm, R. K. Sharma, M. Hein, R. Thoma, "Non-linearly induced interference and its mitigation in cognitive wideband receivers," *18th European Wireless Conference*, pp. 1-6, April 2012

[8] J. Verlant-Chenet, J. Renard, J. Dricot, P. De Doncker, F. Horlin, "Sensitivity of spectrum sensing techniques to RF impairments,"*IEEE Proc. Vehicular Technology Conference*, pp. 1-5, May 2010

[9] A. Zarashi-Ghasabeh, A. Tarighat, B. Daneshrad, "Cyclo-stationary sensing of OFDM waveforms in the presence of receiver RF impairments," *IEEE Proc. WCNC'10*, pp. 1-6, April 2010

[10] R. Tandra, A. Sahai, "SNR walls for signal detection," *IEEE Journal on Selected Topics in Signal Processing*, vol.2, pp. 4-17, Feb. 2008.

[11] J.P.F. Glas, "Digital I/Q imbalance compensation in a low IF receiver", *IEEE Proc. Globecom'98*, vol.3, pp. 1461-1466, 1998.

[12] J. Huettner, S. Reinhardt, M. Huerner, "Low complex I/Q imbalance compensation for low-IF receivers", IEEE Proc. Radio and Wireless Symposium, pp. 303-306, Jan. 2006.

[13] M. Valkama, M. Renfors, V. Koivunen, "Advanced methods for I/Q imbalance compensation in communication receivers," *IEEE Trans. on Signal Processing*, vol. 49, no. 10, pp. 2335-2344, Oct. 2001.